DOI: 10.24996/ijs.2022.63.12.24

ISSN: 0067-2904

Gabbroic Rocks in Mawat Ophiolite Complex, NE Iraq: Geochemical Constraints on their Tectonogenesis

Mohammed A. Al-Jboury*, Omar S. Al-Taweel
Department of Geology, College of Science, University of Mosul, Mosul, Iraq

Received: 6/2/2022 Accepted: 5/6/2022 Published: 30/12/2022

Abstract

The Mawat Ophiolite Complex located in north-eastern Iraq represents part of the Iraqi Zagros Suture Zone, located at the border between the Arabian-Iranian plates. It consists of peridotite, gabbro, subvolcanic sheeted dykes and volcanic pillow lava. The geochemical signatures of the gabbro show a significant variation in major elements concentration, low concentrations of TiO_2 (0.06-0.36 wt.%), Na_2O (0.44-0.98 wt.%), K_2O (0.024-0.48 wt.%), P_2O_5 (0.002-0.009 wt.%) and moderate variations in SiO_2 (46.13-53.77 wt.%) with wide ranges and high concentration of Al_2O_3 (13.87-22.18 wt.%), Fe_2O_3 (0.04-2.95 wt.%), FeO (2.68-8.76 wt.%), MgO (8.09-14.28 wt.%) and CaO (11.08-17.04 wt.%). The flat REE patterns of the present rocks represent island arc tholeiite (IAT) tectonics and a subduction-related environment. The main features of the magma generated in the supra subduction zone are the enrichment of LILEs and depletion of the HFSEs and the strong negative Nb anomaly. Geochemical evidence indicates that the tholeiitic gabbros were generated in an arc-related tectonic setting. The tectonomagmatic diagrams for gabbros and the very low Ti content propose that the gabbroic rocks of Mawat Ophiolite have island arc tholeiitic (IAT) and possibly boninitic affinities which have a related to the supra-subduction zone (SSZ).

Keywords: Gabbro; Mawat, Ophiolite, Tectonogenesis, Iraq.

صخور الكابرو في معقد ماوات الاوفيولايتي، شمال شرق العراق: محددات جيوكيميائية على اصولها التكتونية

محمد احمد الجبوري* ، عمر سيف الدين الطويل
قسم علم الارض، كلية العلوم، جامعة الموصل، الموصل، العراق

الخلاصة

يمثل معقد ماوات الاوفيولايتي الواقع في الجزء الشمالي الشرقي من العراق جزءاً من نطاق الدرز الزاكروسي العراقي على الحدود بين الصفيحتين العربية والإيرانية. يتكون معقد ماوات من صخور البيردوتايت، صخور الكابرو، قواطع من الصخور تحت البركانية، وصخور بركانية وسادية. تظهر السمات الجيوكيميائية لصخور الكابرو تبايناً كبيراً في تراكيز العناصر الرئيسية، تراكيز واطئة من اكاسيد التيتانيوم تتراوح مابين (%

*Email: masuliman@uomosul.edu.iq

0.36–0.06)، الصوديوم (0.98–0.44 %)، البوتاسيوم (0.48–0.024 %) والفسفور (–0.009 %
0.002) ومديات معتدلة في اكاسيد السليكون (53.77–46.13%) ومديات واسعة وتراكيز عالية في الالمنيوم (22.18–13.87 %)، الحديديك (2.95–0.04 %)، الحديدوز (8.76–2.68 %)، المغنيسيوم (14.28–8.09%) والكالسيوم (17.04–11.08 %). يمثل النمط المنبسط للعناصر الارضية النادرة لصخور الدراسة الحالية اقواس الجزر الثولييتية (IAT) في بيئة تكتونية مرتبطة بالغوران. يعد الاغناء بالعناصر ذات القطر الأيوني الكبير (LILE) والافتقار بالعناصر ذات مجال الجذب العالي (HFSE) والشذوذ السالب القوي لـ Nb من السمات الرئيسية للصهارة المتكونة في نطاق فوق الغوران. تشير الادلة الجيوكيميائية الى ان صخور الكابرو هي ثولييتية، وتكونت في بيئة تكتونية مرتبطة بالقوس. توضح المخططات التكتونية والمحتوى المنخفض جدا للتيتانيوم ان صخور الكابرو في معقد ماوات الاوفيولايتي ممثلة صخور الجزر القوسية الثولييتية (IAT) وربما ذو طبيعة بونانيتية مرتبطة بنطاق فوق الغوران.

1. Introduction

A general overview of the geological setting of the Eastern Mediterranean ophiolites indicates that the widespread distribution of depleted basaltic, andesitic, and boninitic lavas prefers the creation of most of the intact large ophiolites above the subduction zone rather than along mid-ocean ridge in the Tethyan region [1]. The several models for the generation of Tethyan ophiolites could be summarised as follows; ophiolites generated along mid-oceanic ridges, ophiolites generated at spreading ridges between microcontinents [2, 3], ophiolites generated at back-arc supra-subduction zone (SSZ) in intra oceanic environments that usually give high magnesium andesite (boninitic) [4, 5], ophiolites developed in fore-arc regions with high magnesium andesite (boninitic) [6]. The peridotites are the lowest members of the ophiolite complexes. At the same time, the oceanic crust is the second member of ophiolites, which comprises volcanic pillow lava, subvolcanic sheeted dykes, and gabbroic rocks [7, 8, 9].

The units of the Zagros Suture Zone were created inside of the Neo Tethys and were thrust over the Arabian Plate during the Late Cretaceous and Miocene-Pliocene [10]. From the southwest, three tectonic zones have been observed in Iraq: Qulqula-Khwakurk, Penjween-Walash, and Shalair zones [9, 11]. The Penjween-Walash Zone includes sequences of volcano-sedimentary that originated in the Cretaceous Neo Tethys spreading, and Paleocene volcanic arc and basic intrusions formed during the ocean's final closure. The Penjween-Walash Zone comprises three thrust sheets: the lower Napurdan, the middle Walash, and the upper Qandil [9, 12, 13, 14]. The upper thrust sheet (Qandil) includes Iraqi ophiolites consisting of Penjween, Mawat, Bulfat, Pushtashan and Hasanbag [15]. The research area lies within the upper Qandil thrust sheet, about 30 km northeast of Sulaimaniya and 4 km north of Chwarta Village in northern Iraq, between latitudes 35° 49´ - 35º 53′ N and longitudes 45° 31´ - 45° 35´ E, (Figure 1). There are just a few studies on the petrogenesis of gabbroic rocks in the Mawat Ophiolite Complex, such as Aqrawi [16], Abdulzahra [17], and Mirza [18], so this paper examines the tectonogenesis of Mawat Ophiolite gabbros depending on petrography and geochemical constraints.

2. General Geology

The Mawat Ophiolite Complex is located 30 kilometres northeast of the city of Sulaimani. The complex is located inside the Penjween-Walash Zone and is part of the Iraqi Zagros Suture Zone (IZSZ) [9]. The complex forms an elongate body that extends about 25 km, striking NE-SW parallel to the Thrust Zone and covering 7 to 12 km, occupying an area of about 250 km^2 [19] (Figure 1). The Iraqi Zagros Suture Zone, according to Aswad [20] is divided into two allochthonous nappes: upper and lower allochthonous, which Al-Mehaidi

[21] called upper and lower thrust sheets. The lower thrust sheet of volcano-sedimentary Palaeogene rocks belonging to the Walash-Naopurdan Group and an upper sheet of Cretaceous metasedimentary and metavolcanic rocks with large ultramafic and mafic bodies [9]. The upper allochthonous (Penjween-Walash Zone) includes the ophiolitic massifs and Gemo-Qandil formations of Albian-Cenomanian [22], It is also named as ophiolite bearing terranes [12]. The lower allochthonous represents the lower transported nappes above the passive margin. The ophiolite is composed of the upper thrust sheet (Mawat Nappe), which is 600-1000 m thick and consists of basaltic rocks called as Mawat Group, which is intruded by ultrabasic, coarse and layered gabbros, diorites, subvolcanic dykes and plagiogranite [19], and overlaid by a Gimo Group (interbedded basalt and marble).

Gabbro is situated in the central part of the ophiolite, with a thickness of about 1000 m. The Mawat Ophiolite Complex is dominated by gabbro [19], followed by ultrabasic rocks (dunite, harzburgite, lherzolites, and pyroxenite) and diorite and diabase intrusions [19]. Gabbro member consists of banded amphibolized gabbro, metagabbro, pyroxene gabbro, greenschist, albite and epidosite amphibolites [19, 21]. Banded gabbro is the largest body intruded in the east by coarse gabbro that outcrops at the east thrust contact. The banded gabbro western contact with greenschist is a North-South trending shear zone where the gabbro is firmly crushed and deformed and is intruded by minor acidic and basic intrusions [9].

3. Materials and Methods

Samples are carefully selected on petrographic criteria to ensure that a complete range of compositions is obtained. They are prepared for chemical analysis, starting by crushing in a jaw crusher. The surface parts affected by weathering processes were cleaned and removed, and then the fresh parts were powdered using a time swing mill to the size of less than 63 mesh. Then 1 gm of the powder of each sample was heated to 1100 ºC for 2 h to determine the LOI in the Department of Geology, Mosul University laboratories. Eleven samples of layered gabbros are analysed for major, trace, and rare earth elements (REE) by ACME Analytical Laboratories Ltd., Vancouver, Canada, using ELAN 6000 ICP-MS. Before ICP-MS analysis, however, the whole rock powders (0.25 mg) were digested with an acid mixture of H_2O_2-HF-$HClO_4$-HNO_3 (multi-acid digestion), then heated on a hot plate until the fumes came out and then left to cool. They were finally dissolved in 5% HCl. Because (ICP-MS) analysis could not distinguish iron oxide (FeO) from ferric oxide (Fe_2O_3), it had to be measured separately at the Mosul University using an ECIL CE 3021 spectrometer using Jeffery and Hutchison [23] procedure (Tables 1, 2).

4. Petrology and Petrography

The gabbro member is located in the central part of the ophiolite with a thickness of about 1 km. It is the major part of the Mawat Ophiolite Complex, and it occupies around 170 km^2 of the complex [19]. The research area includes three types of gabbros, according to a previous study done by Abdulzahra [17], and Al-Saffi et al. [24]: layered gabbro, dyke pegmatoid gabbro and marginal gabbro. Abdulzahra [17], and Al-Saffi et al. [24] suggested that these rocks exhibit three types of deformation: crystal-plastic, semi-brittle, and brittle deformations. The gabbroic rock samples were collected by Aqrawi [16] and Zekaria [25] during the fieldwork.

The textures of these rocks are often granular and porphyroclastic (Plate 1 a, b), although they can also have a schistosity texture (Plate 1 c). Hatch et al. [26] suggested that in schistose and sheared rocks, many feldspars are granulated and crushed to smaller sizes, and secondary amphiboles replaced most pyroxenes. According to Al-Hassan [27], the schistose of Penjween gabbroic rocks indicates the emplacement and thrust. These rocks are composed of plagioclase, amphibole uralitized with relict pyroxene, minor chlorite, and opaques. Gabbro also has an ophitic and sub-ophitic texture, showing that plagioclase crystals are entirely or partially enclosed within secondary amphibole (Plate 1 d). Plagioclase is moderately sericitized and is mostly labradorite (An_{62}-$_{65}$). Plagioclase has largely suffered granulation, which changes shape and grain size, and its form varies from subhedral to anhedral, affected by crushing and granulation (Plate 1 b). Tectonic deformations such as granulated, wavy extinction, fractured, bent lamellae, and kink banding are shown in plagioclase (Plate 1 e). Plagioclase exhibits the most severe alteration in shear zones, where grains may be replaced by small calcite and epidote due to the saussuritization process (Plate 1 f). Plagioclase with tails of polygonal neoblasts (Plate 1 b) can be seen in some of the most strongly deformed samples, indicating that crystal plastic deformation has ended and semi-brittle deformation has started [24]. Pyroxene is usually augite (extinction angle 41) which is uralitized in varying degrees (Plate 1 g). There are two types of amphibole: primary (Plate 1 h) and secondary amphibole. The Latter resulting from uralitisation of the primary pyroxene contents occur mainly in the shear zones where the rocks have been deformed along their contact with dunite (Plate 1 g).

5. Results

5.1 Major Oxides

On the CaO-Al_2O_3-MgO diagram [28], the gabbroic rocks of Mawat Ophiolite Complex are located in the cumulate mafic rocks (Figure 2 a). The silica and total alkalis (TAS) diagram [29] shows that these rocks are tholeiitic/sub-alkaline gabbros (Figure 2 b). The tholeiitic character of all rocks is confirmed by the YTC and Zr-Y diagrams (Figure 2 c, d). The whole rock analysis show moderate variations in SiO_2 (46.13-53.77 wt.%) and low concentrations of TiO_2 (0.06-0.36 wt.%), Na_2O (0.44-0.98 wt.%), K_2O (0.024-0.48 wt.%), P_2O_5 (0.002-0.009 wt.%) and wide ranges and high concentration of Al_2O_3 (13.87-22.18 wt.%), Fe_2O_3 (0.04-2.95 wt.%), FeO (2.68-8.76 wt.%), MgO (8.09-14.28 wt.%) and CaO (11.08-17.04 wt.%) (Table 1). The concentrations of CaO, MnO, and Na_2O exhibit positive correlations with MgO, while the behaviour of FeO, Al_2O_3, and TiO_2 show negative correlations with MgO, while SiO_2, Fe_2O_3, K_2O, and P_2O_5 for all samples show scattered correlations (Figure 3). Most of the scattered results in Figure 3 can be attributed to the layering nature of gabbros and the alteration process.

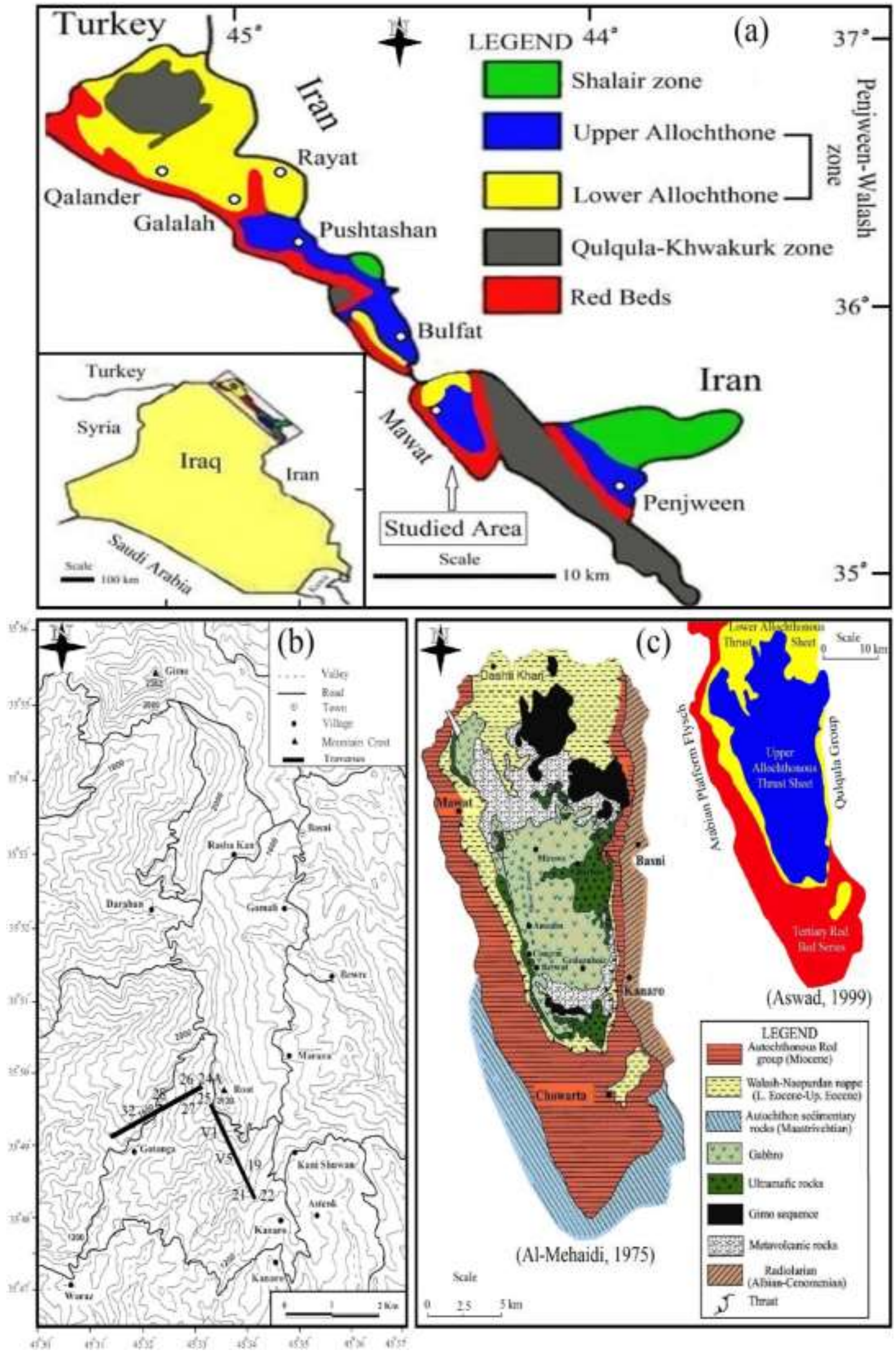

Figure 1: (a) Geological map of the Iraqi Zagros Suture Zone (IZSZ) shows the site of the studied area. (b) Topographic map of the study area (c) Geological map of Mawat Ophiolite Complex, northeastern Iraq [21, 20].

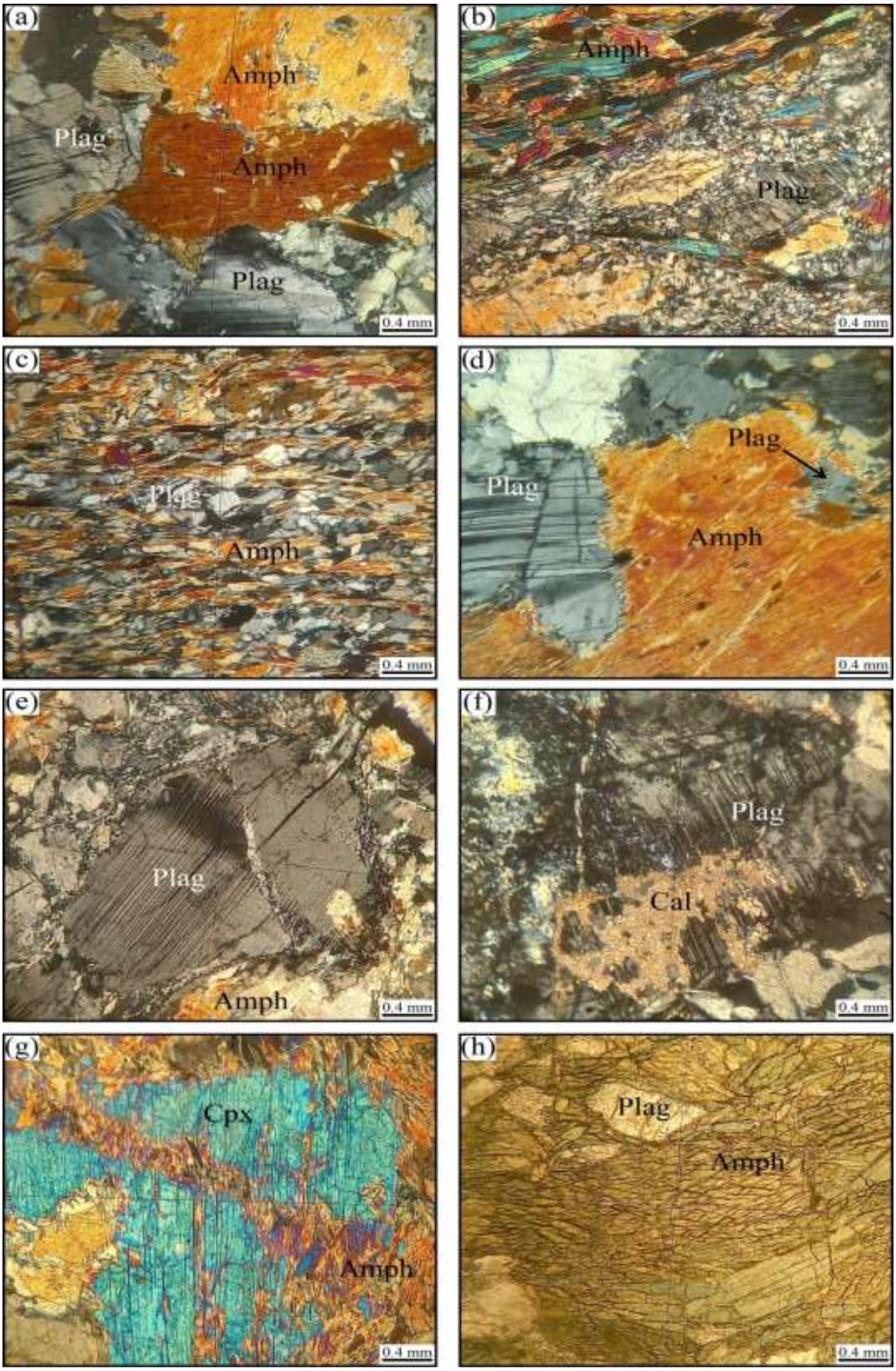

Plate 1- Photomicrographs showing (a) Gabbro show granular textures, sample, 32. (b) Gabbro show porphyroclastic texture and granulation, sample V5. (c) Schistosity texture in gabbro, sample 19. (d) Ophitic and sub-ophitic texture, sample 32. (e) Plagioclase shows kink banding, sample 26. (f) Calcite formed as a result of saussuritization of plagioclase, sample 28. (g) Secondary amphibole formed as a result of uralitization of clinopyroxene, sample 24A.

(h) Primary amphibole has a prismatic cleavage angle about 56° and 124°, sample, 21, [Pl : Plagioclase; Cpx: Clinopyroxene; Amph: Amphibole; Cal: Calcite].

Table 1: Content of major and trace elements in gabbroic rocks from the Mawat Ophiolite

	Sample No.	V1	V5	32	28	27	26	25	24A	22	21	19
Major oxides (wt%)	SiO_2	51.44	51.61	51.64	49.36	53.78	47.22	49.39	46.82	48.15	48.68	**46.16**
	TiO_2	0.25	0.28	0.19	0.36	0.11	0.11	0.13	0.13	0.14	0.07	**0.06**
	Al_2O_3	14.79	15.21	16.83	16.55	15.92	16.66	14.92	13.87	14.07	15.02	**22.18**
	FeO	7.00	7.33	5.55	8.76	3.87	2.68	3.27	6.02	5.55	4.08	**2.83**
	Fe_2O_3	0.75	0.83	0.79	0.04	0.57	2.94	2.45	0.44	0.31	0.84	**1.62**
	MnO	0.18	0.16	0.15	0.19	0.11	0.13	0.13	0.15	0.14	0.13	**0.11**
	MgO	11.47	10.36	10.01	9.24	10.76	11.92	12.34	14.28	13.03	13.61	**8.09**
	CaO	11.08	11.23	11.99	13.60	12.00	15.24	14.63	14.65	15.70	14.38	**17.04**
	Na_2O	0.98	0.85	0.65	0.70	0.44	0.50	0.44	0.56	0.48	0.49	**0.51**
	K_2O	0.05	0.04	0.04	0.05	0.02	0.02	0.05	0.04	0.02	0.04	**0.02**
	P_2O_5	0.005	0.01	0.005	0.01	0.01	0.005	0.002	0.005	0.002	0.007	**0.002**
	LOI	2.00	2.10	2.20	1.20	2.40	2.60	2.30	3.10	2.40	2.70	**1.40**
	Total	99.9	100.01	99.9	99.9	100.01	99.9	100.01	99.9	99.9	99.9	**100.01**
Trace element (ppm)	Ni	118	96.0	107.2	89.4	138.1	151.7	143.2	173.3	169.1	161.6	**110.4**
	Cr	153	193	141	139	218	223	261	164	270	277	**122**
	Sc	50.7	50.6	44.1	48.3	34.4	43.1	47.8	50.2	52.7	42.8	**24.8**
	V	241	273	134	278	137	150	155	174	179	134	**103**
	Ba	13.0	8.00	10.0	4.00	3.00	3.00	5.00	3.00	9.00	34.0	**4.00**
	Rb	0.60	0.20	0.10	0.60	0.60	0.40	0.20	0.40	0.40	0.50	**0.70**
	Sr	142	143	84.0	84.0	58.0	64.0	64.0	57.0	62.0	66.0	**141**
	Zr	5.20	4.20	2.10	1.90	4.20	1.00	1.70	1.20	1.20	0.60	**0.30**
	Y	6.10	7.40	13.0	8.10	1.70	2.70	3.80	3.20	3.60	1.70	**1.10**
	Nb	0.20	0.20	0.10	0.08	0.08	0.04	0.08	0.05	0.07	0.06	**0.08**
	Ga	10.59	11.21	11.48	12.44	9.40	9.49	9.40	8.76	9.24	8.51	**11.57**
	Cu	2.50	12.56	10.15	50.01	8.98	56.27	60.64	8.21	10.26	1.90	**4.37**
	Zn	50.80	56.30	47.9	66.8	24.3	32.5	73.7	37.5	36.3	26.3	**20.3**
	Pb	0.39	0.42	0.47	0.36	0.33	0.31	0.31	0.38	0.52	0.27	**0.36**
	Mo	0.19	0.32	0.12	0.32	0.16	0.49	0.09	0.09	0.35	0.09	**0.41**
	Co	58.50	55.8	45.8	53.1	47.7	52.4	52.8	62.5	56.4	51.2	**43.3**
	As	0.80	1.50	0.40	1.90	0.30	0.30	1.40	1.10	1.40	0.20	**1.20**
	Au	<0.10	<0.10	<0.10	<0.10	<0.10	<0.10	<0.10	<0.10	<0.10	<0.10	**<0.10**
	Cd	0.06	0.06	0.13	0.09	0.11	0.09	0.07	0.09	0.14	0.11	**0.12**
	Sb	0.06	0.07	0.03	0.03	0.11	0.03	0.03	0.07	0.05	0.18	**0.08**
	Bi	<0.04	<0.04	<0.04	<0.04	0.07	<0.04	<0.04	<0.04	<0.04	<0.04	**0.05**
	W	75.90	70.3	75.10	58	129.2	43.0	63.8	61.1	76.8	77.10	**71.4**
	Sn	<0.10	0.20	0.10	<0.10	0.10	<0.10	<0.10	<0.10	<0.10	<0.10	**<0.10**
	Be	<1.00	<1.00	<1.00	<1.00	<1.00	<1.00	<1.00	<1.00	<1.00	<1.00	**<1.00**
	Li	1.70	1.10	0.80	1.10	0.80	1.10	0.80	1.40	1.60	2.10	**0.50**

5.2 Trace and Rare Earth Elements

Large ion lithophile (LIL) elements (in ppm) like Sr (57-143), Ba (3-34), Rb (0.1-0.7), and Ce (0.15-1.18), and High Field Strength (HFS) elements (in ppm) like Zr (0.3-5.2), Y (1.1-13), and Nb (0.04-0.2) (Table 1) have varying concentrations in the Mawat gabbros. As a result, LIL elements (Sr, Ba, Rb, and K) are likely to have been remobilised to varying degrees throughout alteration processes [30].

The binary variation diagrams use Zr against major oxides and trace elements because Zr is supposed to be immobile [31]. Figure 4 shows Zr against HFS elements (Nb, Y, and Ti). It illustrates a linear correlation with some dispersed resulting from cumulate phases. Figure 4 refers to all these gabbros are may be created from one melt and one origin during fractionation because the HFS elements are less influenced by secondary alteration [32]. Zircon (Zr) has a positive correlation with SiO_2 and Ti but a negative correlation with MgO. Early crystallised minerals, including pyroxene and calcic plagioclase formed throughout magma differentiation; therefore, the negative connection of MgO with Zr makes sense [18]. On the other hand, Ni and Cr negatively correlate with Zr, which causes plagioclase and clinopyroxene to crystallise during the magma differentiation [33]. Wilson [34] proposes using the variations trend of Zr against SiO_2, La, Ga, Y, and Ce to investigate the fractional crystallisation processes in basic rocks (Figure 4).

Table 2- Content of REE elements (in ppm) in gabbroic rocks from the Mawat Ophiolite

	Sample No.	V1	V5	32	28	27	26	25	24A	22	21	19
Rare earth element (ppm)	La	0.40	0.40	0.30	0.20	0.10	0.20	0.10	0.20	0.20	0.10	**0.50**
	Ce	0.86	1.18	1.06	0.56	0.20	0.25	0.32	0.26	0.29	0.15	**0.15**
	Pr	0.20	0.30	0.30	0.10	<0.10	<0.10	<0.10	<0.10	<0.10	<0.10	**0.10**
	Nd	1.00	1.00	1.70	10.00	0.10	0.30	0.40	0.30	0.40	0.20	**0.10**
	Sm	0.50	0.50	0.80	0.60	0.10	0.20	0.30	0.20	0.20	<0.10	**<0.10**
	Eu	0.20	0.20	0.30	0.30	<0.10	0.10	0.10	0.10	<0.10	<0.10	**<0.10**
	Gd	0.50	0.80	1.40	1.20	0.20	0.40	0.50	0.40	0.50	0.20	**0.30**
	Tb	0.10	0.20	0.30	0.20	<0.10	<0.10	<0.10	<0.10	<0.10	<0.10	**<0.10**
	Dy	1.00	1.20	2.90	1.60	0.40	0.60	0.80	0.70	0.70	0.30	**0.20**
	Ho	0.30	0.30	0.50	0.40	<0.10	0.10	0.20	0.10	0.20	<0.10	**<0.10**
	Er	0.60	1.00	1.70	1.00	0.20	0.30	0.50	0.40	0.50	0.20	**0.20**
	Tm	<0.10	0.10	0.20	0.10	<0.10	<0.10	<0.10	<0.10	<0.10	<0.10	**<0.10**
	Yb	0.70	0.90	1.30	0.90	0.20	0.40	0.50	0.40	0.40	0.20	**0.10**
	Lu	<0.10	0.10	0.20	0.20	<0.10	<0.10	<0.10	<0.10	<0.10	<0.10	**<0.10**
Other	Cs	0.10	0.20	<0.10	<0.10	<0.10	<0.10	<0.10	<0.10	<0.10	0.10	**<0.10**
	Hf	0.20	0.20	0.13	0.09	0.12	0.05	0.04	0.07	0.04	0.03	**0.03**
	Th	0.12	0.10	0.13	0.10	0.10	0.13	0.12	0.10	0.10	0.10	**0.12**
	U	<0.10	<0.10	<0.10	<0.10	<0.10	<0.10	<0.10	<0.10	<0.10	<0.10	**<0.10**
$(REE Ratio)_N$	$(La/Sm)_N$	0.52	0.52	0.24	0.22	0.65	0.65	0.22	0.65	0.65	-	**-**
	$(La/Yb)_N$	0.41	0.32	0.17	0.16	0.36	0.36	0.14	0.36	0.36	0.36	**3.59**
	$(Gd/Yb)_N$	0.59	0.74	0.89	1.10	0.83	0.83	0.83	0.83	1.03	0.83	**2.48**
	$(Ce)_N/Ce^*$	0.76	1.05	0.84	0.72	0.93	0.53	0.92	0.55	0.56	0.58	**0.17**

The parallel and flat REE patterns of these rocks indicate that they have originated from the same source. Light rare elements LREE depletion [$(La/Sm)_N$ = 0.22-0.65], [$(La/Yb)_N$ = 0.14-0.41, except sample 19 =3.59], as well as flat middle MREE and heavy HREE patterns

[$(Gd/Yb)_N$ = 0.59- 1.1], except sample 19 = 2.48], can be seen in the chondrite-normalized REE patterns (Figure 5 a). Gabbros have flat REE patterns with negative Ce anomaly (Ce_N/Ce^* [$Ce^* = (2\times La_N+Nd_N)/3$] = 0.17-1.05) and no Eu anomaly in their overall patterns.

The multi-element patterns on the spider diagram are similar in all samples, indicating that they evolved from a single magmatic source. The relative enrichment of LILE relative to HFSE is shown in this diagram (Figure 5 b). This diagram is characterised by the positive anomalies of Rb, Sr, Ba, and K relative to Nb, Hf and Zr. The enrichment in LILE with HFSE depletion and a conspicuous negative Nb, Ti, and Zr anomaly are thought to be typical of subduction zone basaltic rocks [34, 35]. Enrichment in LILE and depletion in HFSE are characteristics of gabbros of ophiolite complex and dykes of tholeiite to boninite affinities in the subduction zone [36].

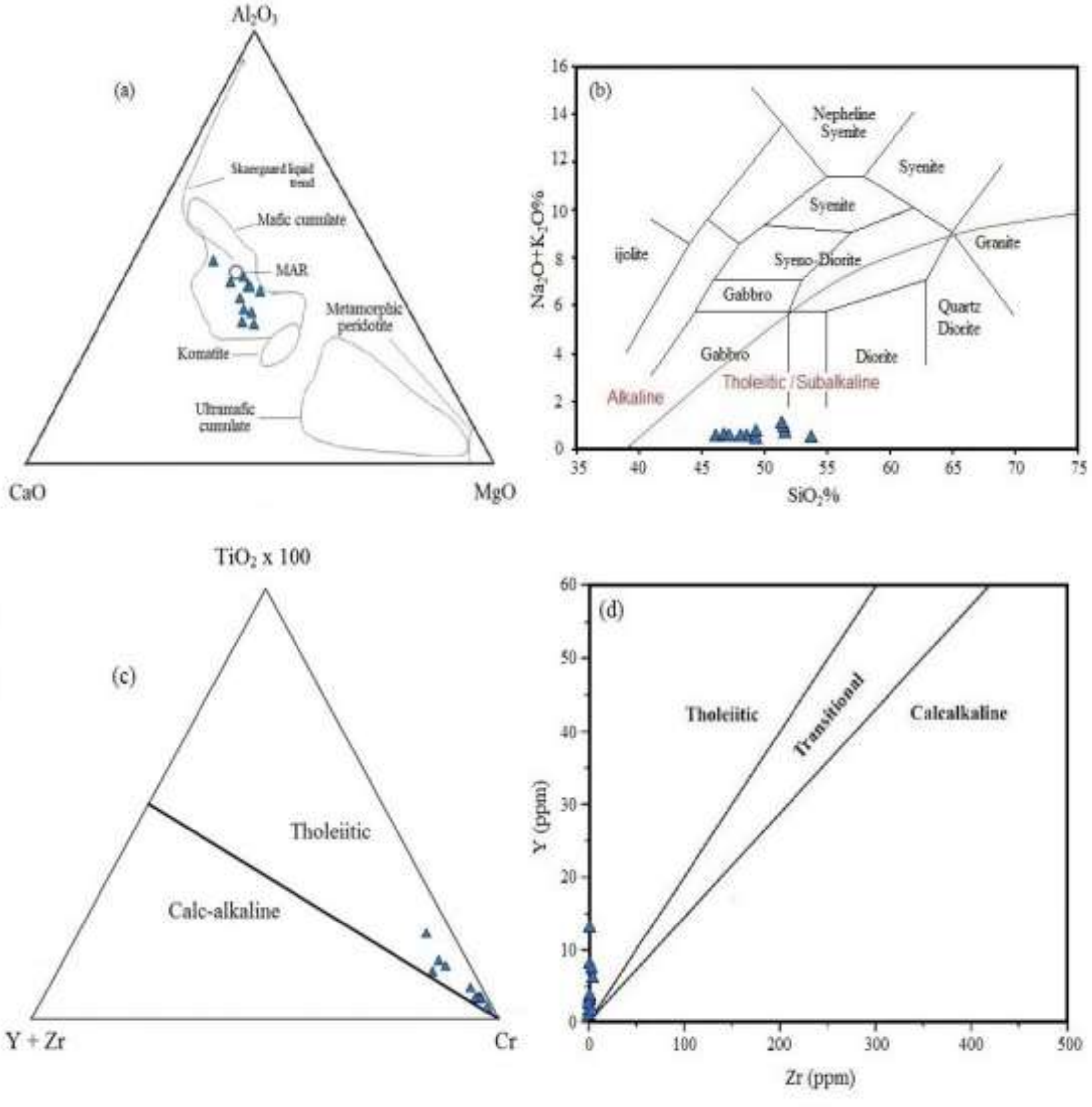

Figure 2: Mawat Ophiolite gabbro geochemical classifications (a) CaO-Al_2O_3–MgO ternary diagram of gabbros from the Mawat Ophiolite [28], MAR is the mid-Atlantic ridge average composition. (b) SiO_2-(Na_2O+K_2O) diagram [29] for geochemical classification of the analysed samples. (c) YTC ternary diagram [37] of Mawat Ophiolite gabbros. (d) Zr-Y diagram [38].

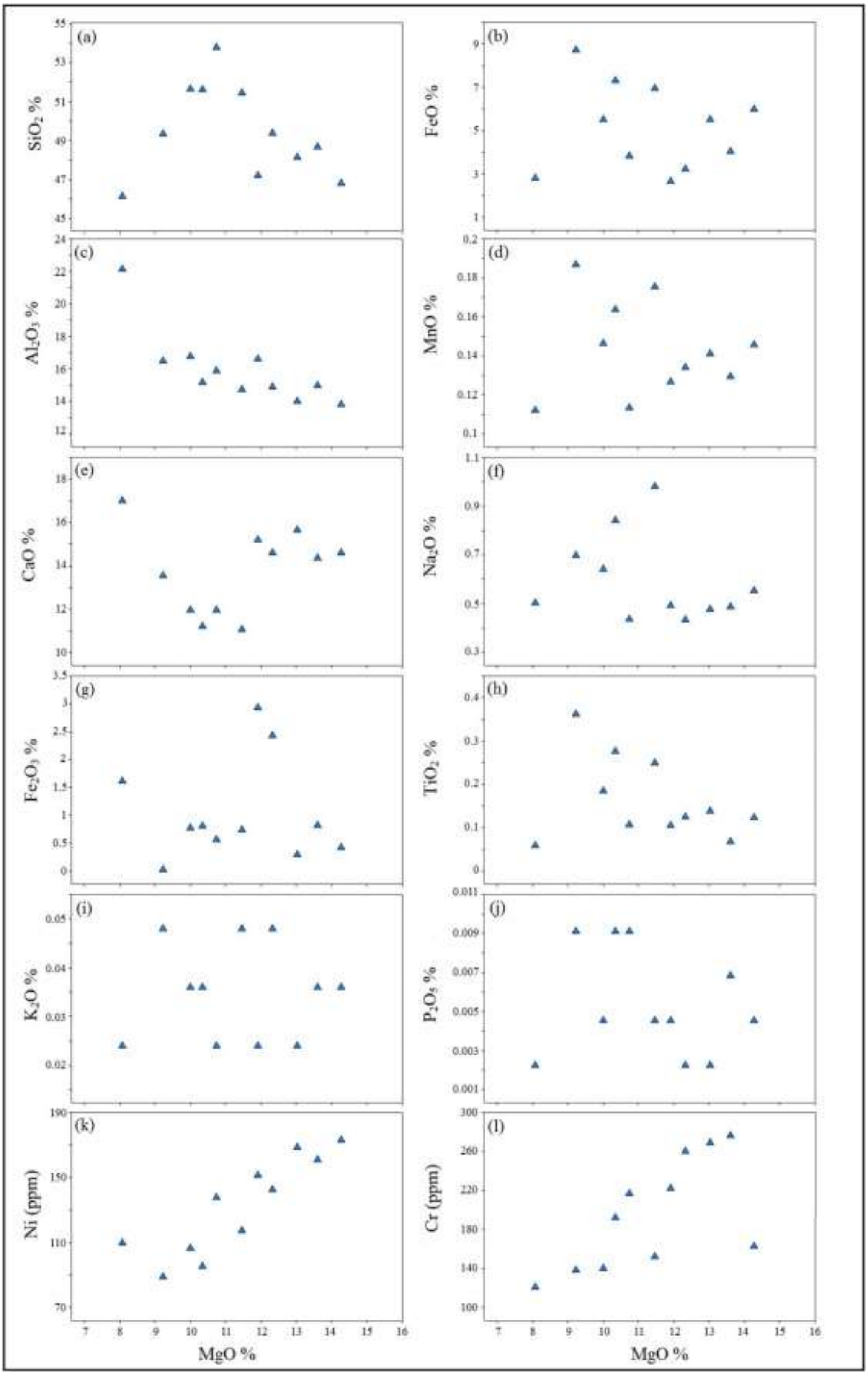

Figure 3: MgO vs selected major and trace elements plots of the Mawat gabbros.

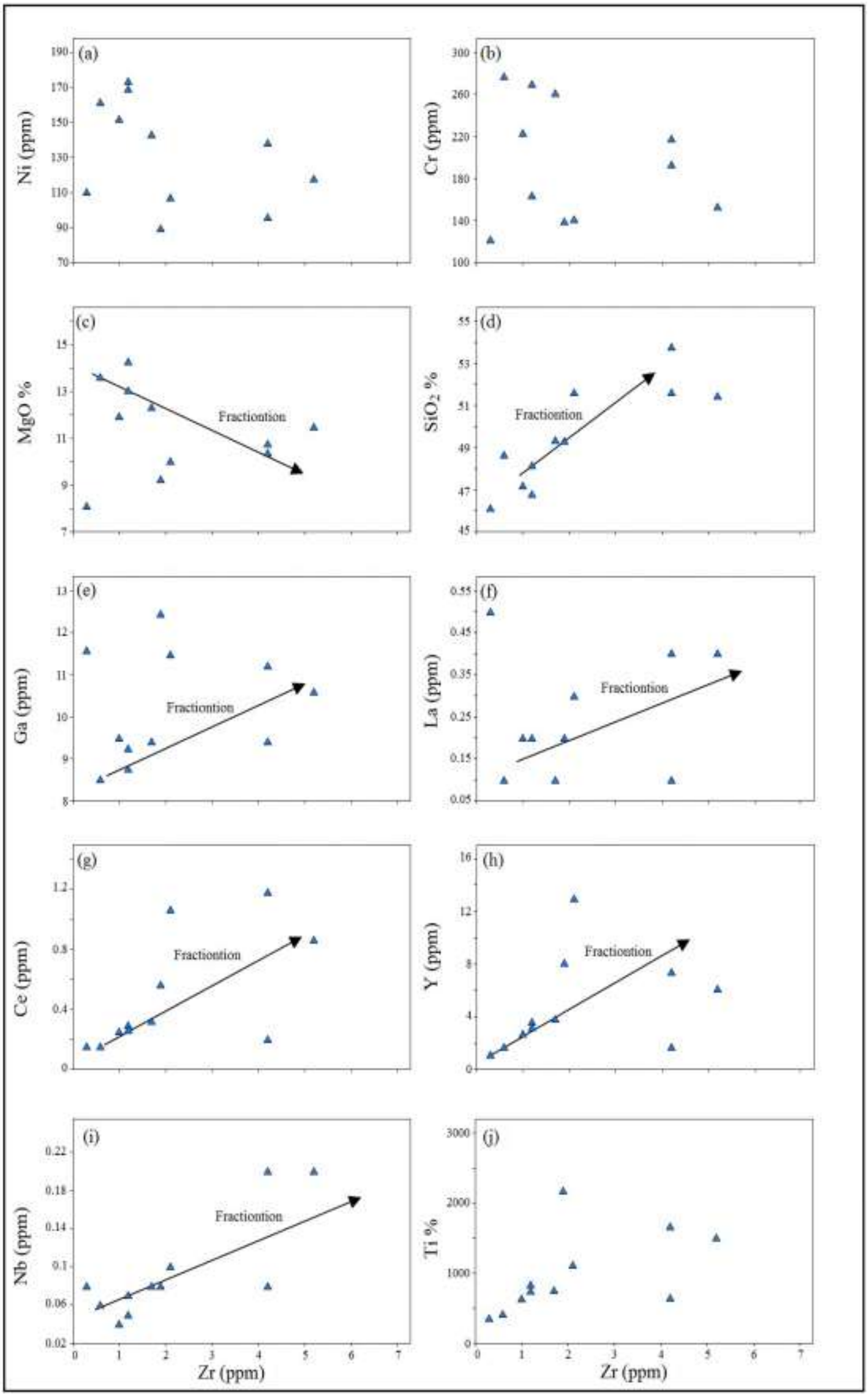

Figure 4: Zr (ppm) vs selected elements plots of the Mawat gabbros, the trends from Wilson [34].

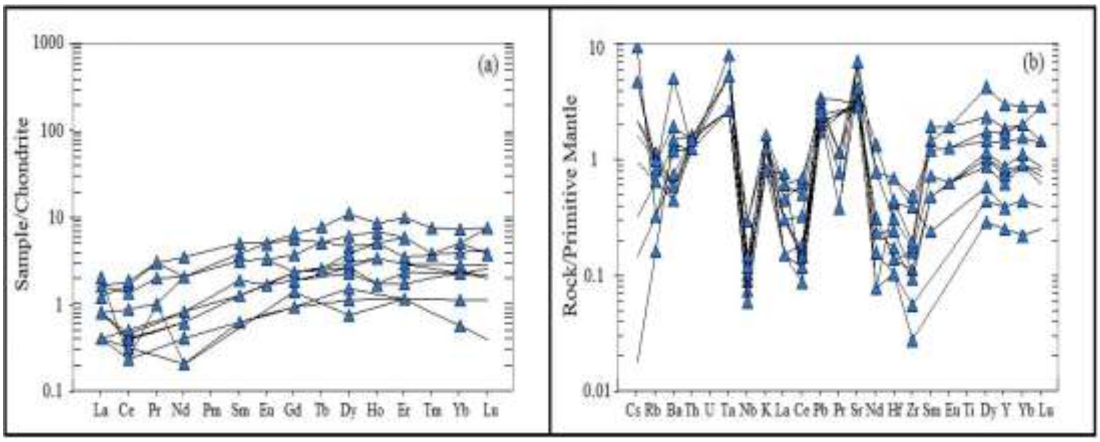

Figure 5: (a) Chondrite normalised REEs patterns of Mawat Ophiolite gabbros [39]. (b) Primitive mantle normalised multi-element diagram of Mawat Ophiolite gabbros [39].

6. Discussion

The geochemical composition of Mawat Ophiolite gabbros indicates the fractional crystallisation of Ca-plagioclase. The relation between Cr and Ni is used to predict magma evolution and identify the minerals that will crystallise first. When the Mawat gabbro rock samples are projected onto the Figure (6 a), it is clear that they form a linear relationship parallel to clinopyroxene with plagioclase dispersion. This diagram shows that clinopyroxene crystallised first instead of olivine. Clinopyroxene developed as the first phase in mafic rocks, based on the more significant Cr depletion compared to Ni [40]. In Pearce and Flower's [41] diagrams (Figure 6 b, c), the gabbros are shown to have formed by fractional crystallisation with pathways parallel to clinopyroxene and plagioclase.

Th-Zr-Nb and Y-Nb/Th diagrams show that these gabbroic rocks are plotted in the island arc tholeiite arc-related magma settings, respectively (Figure 7 a, b). Most gabbros fall into the arc-related cumulate mafic field when major element concentrations are projected on Beard's [42] AFM diagram (Figure 7 c). This implies that these rocks formed in the magma chamber due to crystal fractionation of primary magma through a depleted mantle. This indicates the gabbroic rocks originated in a supra subduction zone [43]. Beccaluva et al. [44] proposed the Ni-Ti/Cr diagram to distinguish between very low Ti basalt (boninites), island arc tholeiite (IAT), and mid-ocean ridge basalt (MORB) by using the relation between the incompatible element (Ti) with compatible elements (Ni and Cr). Mawat gabbroic rocks are classified as very low-Ti basalts (boninite) (Figure 7 d).

The REE patterns of gabbros in the Mawat Ophiolite Complex (Figure 5 a) are similar to those observed in subduction-related and island arc tholeiitic (IAT) rocks [45]. Gabbros are slightly enriched in MREE and HREE and depleted in LREE, with relatively flat REE patterns. The flat and parallel REE patterns of the Mawat gabbros may suggest that they formed from the same depleted mantle source, which may have been dominated by dunite and harzburgite with local occurrences lherzolite [46]. The multi-element patterns of gabbros in the Mawat Ophiolite Complex (Figure 5 b) show Sr and Ba enrichment but a lack of enrichment of Zr and Y; these patterns, along with HFSE variations in tholeiitic rocks, are typical of a supra subduction environment [47]. The enrichment in LILE (compared to primitive mantle) in the gabbroic rocks of Mawat is considered to have been derived from the mantle source region metasomatised by subducted sediment and subduction zone fluid [36]. Depletion of HFS elements such as Zr, Nb, Th and Hf refers to LILE separation such as Sr, Ba, Rb, and HFS elements during subducting slab dehydration [48]. The negative Nb anomaly and the enrichment in LILE compared with the depletion in HFSE spider diagram patterns are typical for supra-subduction magmas [49].

These gabbros are located inside a boninitic field on the MnO-TiO_2-P_2O_5, Zr-Ti, and Ti-V tectonomagmatic diagrams, confirming their formation in a subduction zone. (Figure 8 a, b, c). A significant IAT and boninitic character can be seen in the magmatic rocks of an ophiolitic assemblage in a subduction zone [50]. The TiO_2 concentration of boninite (<0.5%) is lower than that of IAT (<1%) [45]. In comparison, Mawat Ophiolite gabbros have very low TiO_2 contents (0.06–0.36%) as Ali and Rostum [46] demonstrated in the Penjween gabbros and are thus possibly formed from magmas with a boninite-like composition (Figure 8 d). The ophiolites are divided into two types: magmatic island arc (low-Ti) and boninite (very low-Ti), which form in supra-subduction zone settings [51]. As a result, the Mawat gabbros are related to the island arc tholeiite (IAT) and boninite rocks, which are related to the supra-subduction zone.

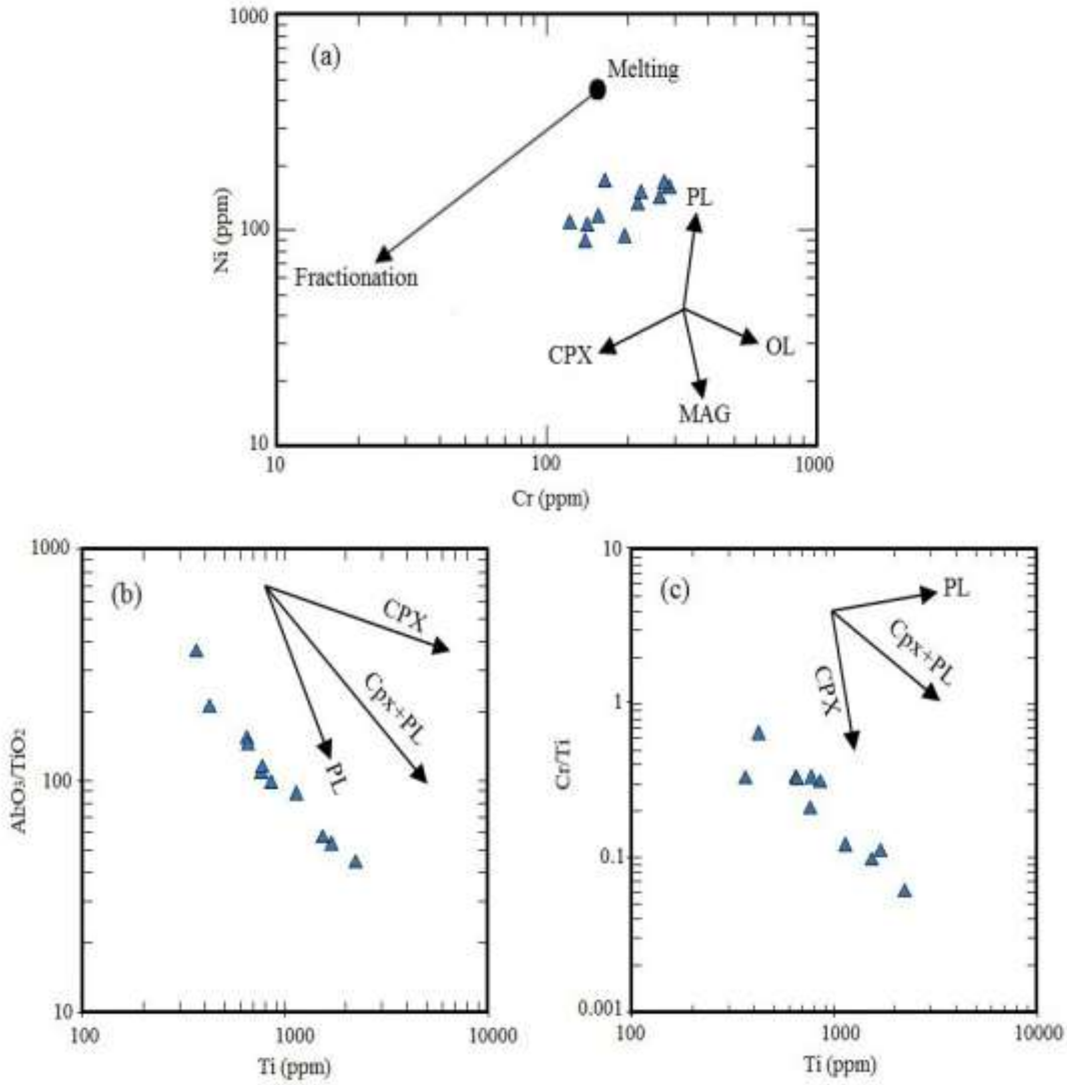

Figure 6: (a) Ni-Cr shows the fractionation. (b) Ti-Al2O3/TiO2 diagram for the Mawat gabbroic rocks [41]. (c) Ti-Cr/Ti diagram for the Mawat gabbroic rocks [41].

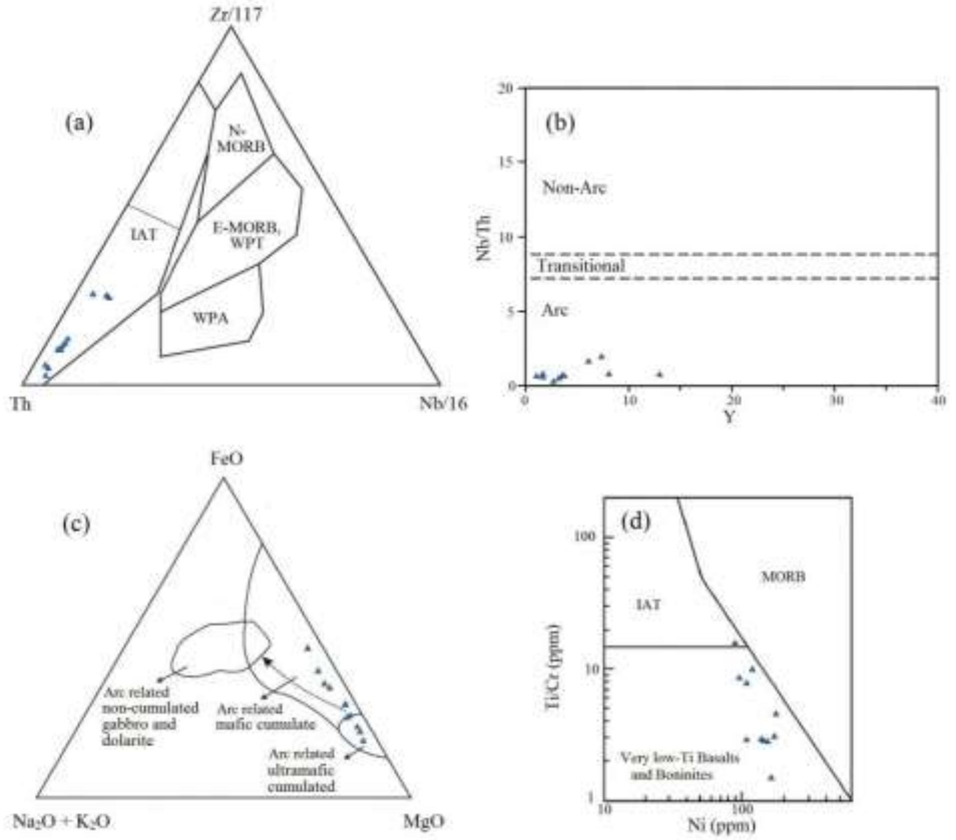

Figure 7: (a) Th-Zr-Nb ternary diagram of gabbroic rocks from Mawat Ophiolite [52]. (b) Y-Nb/Th plot [53]. (c) AFM ternary diagram of gabbroic rocks from Mawat Ophiolite [42], the arrow represents fractional crystallization. (d) Ni-Ti/Cr diagram of gabbroic rocks from Mawat Ophiolite [44].

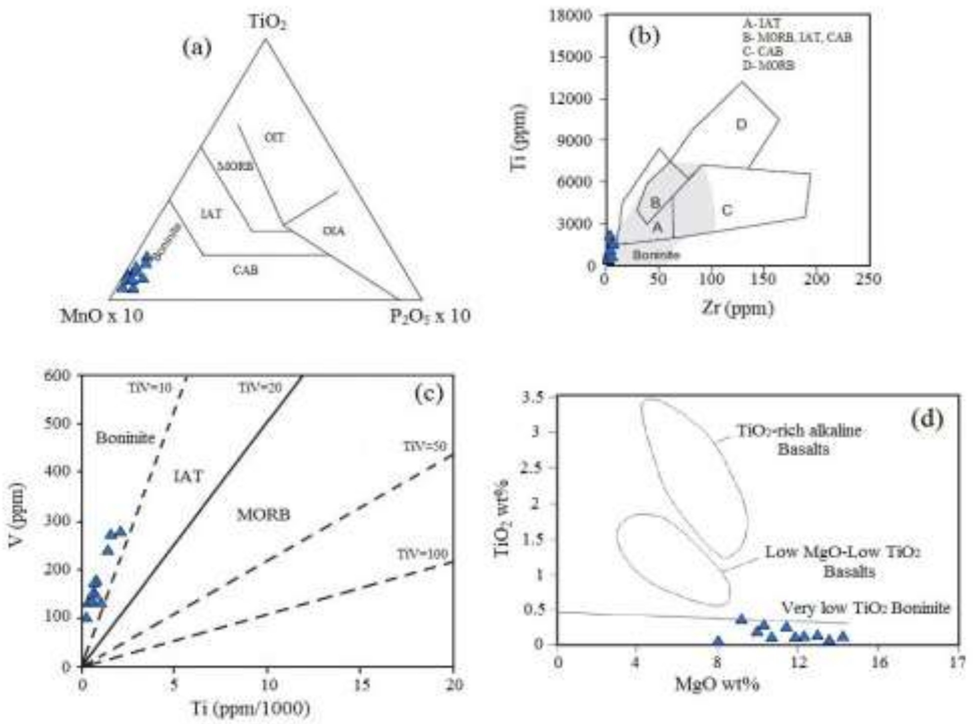

Figure 8: (a) MnO-TiO2-P2O5 diagram [54]. (b) Zr-Ti diagram [55], the shady field in Johnson and Fryer [56]. (c) Ti-V diagram [57]. (d) MgO- TiO2 diagram [58].

7. Conclusions

Gabbro is the major part of the Mawat Ophiolite Complex, followed by ultrabasic rocks and smaller diorite and diabase intrusions. The textures of these rocks are often granular and porphyroclastic, although they can also have a schistosity texture. Gabbros described here are of the island arc thoelittic type, and they formed in the magma chamber as a result of crystal fractionation of primary magma through the depleted mantle. The REE and multi-element patterns of gabbros in the Mawat Ophiolite Complex imply a supra-subduction environment. Since Mawat Ophiolite gabbros have very low TiO_2 contents, these rocks are thought to have island arc tholeiitic (IAT) and maybe boninitic affinities, which are related to the supra-subduction zone (SSZ).

Acknowledgements

The authors are very grateful to the College of Sciences, the University of Mosul, for their provided facilities, which helped improve this work's quality. So, we would like to thank Dr Azzam H. Al-Samman for his helpful and constructive review, which improved the manuscript. The authors are very grateful to the Editor in Chief, the Secretary of the Journal and the Technical Editors for their outstanding efforts and valuable comments.

References

[1] A.H.F. Robertson, "Overview of the Genesis and Emplacement of Mesozoic Ophiolites in the Eastern Mediterranean Tethyan region," *Lithos*, vol. 65, pp. 1-67, 2002.

[2] R. Hall, "Ophiolites: Fragments of Ophiolitic Lithosphere," *Geological Society, London, Special Publications*, vol. 13, pp. 393-404, 1984.

[3] Y. Dilek, P. Thy, B. Hacker and S. Grundvig, "Structure and Petrology of Tauride Ophiolites and Mafic Dike Intrusions (Turkey): Implications for the Neotethyan ocean," *Geological Society of America Bulletin*, vol. 111, pp. 1192-1216, 1999.

[4] A. Miyashiro, *Metamorphism and Metamorphic Belts, George Allen and Unwin Limited, London*, 1973, p. 492.

[5] J.A. Pearce, T. Alabaster, A.W. Shelton and M.P. Searle, "The Oman Ophiolite as a Cretaceous Arc-Basin Complex; Evidence and Implications," *Philosophical Transactions of the Royal Society of London*, vol. 300, pp. 299-317, 1981.

[6] M. Rabinowicz, G. Ceuleneer and A. Nicolas, "Melt Segregation and Flow in Mantle Diapirs below Spreading Center: Evidence from the Oman Ophiolite," *Journal of Geophysical Research*, vol. 92, pp. 3475-3486, 1987.

[7] Y. Dilek and P. Thy, "Structure, Petrology and Seafloor Spreading Tectonics of Kizildag Ophiolite, Turkey," *Geological Society, London, Special Publications*, vol. 148, pp. 43-69, 1998.

[8] E.M. Kleine, "Geochemistry of the Igneous Oceanic Crust," *Elsevier-Pergamon, Oxford*, vol. 3, pp. 433-464, 2004.

[9] S.Z. Jassim and J.C. Goff, *Geology of Iraq, Dolin, Prague and Moravian Museum, Brno*, 2006, p. 341.

[10] S.M. Awadh, and Y. Kettanah, "Petrology, Geochemistry and Tectonical Environment of the Shalair Metamorphic Rock Group and Kata Rash Group, Shalair Valley Area, Northestern Iraq," *Iraqi Journal of Science*, vol. 49, no. 1, pp. 149-158, 2008.

[11] I.K. Abdulzahra and A. Hadi, "Petrology of the Granitoid Intrusions in the Shalair Valley Area, Northeastern Iraq," *Iraqi Journal of Science*, vol. 58, no.1A, pp. 88-102, 2017.

[12] K.J. Aswad, N.R. Aziz and H.A. Koyi, "Cr-spinel Compositions in Serpentinites and their Implications for the Petrotectonic History of the Zagros Suture Zone, Kurdistan Region, Iraq," *Geological Magazine*, vol. 148, no. (5–6), pp. 802–818, 2011.

[13] S.A. Ali, S. Buckman, K.J. Aswad, B.G. Jones, S. Ismail and A.P. Nutman, "Recognition of Late Cretaceous Hasanbag Ophiolite Arc Rocks in the Kurdistan region of the Iraqi Zagros Thrust Zone: A missing Link in the Paleogeography of the Closing Neo–Tethys Ocean," *Lithosphere*, vol. 4, pp. 395-410, 2012.

[14] S.A. Ali, S.A. Ismail, A.P. Nutman, V.C. Bennett, B.G. Jones and S. Buckman, "The Intra-Oceanic Cretaceous (˜108 Ma) Kata-Rash Arc Fragment in the Kurdistan Segment of Iraqi Zagros Suture Zone: Implications for Neotethys Evolution and Closure," *Lithos*, vol. 260, pp. 154-163, 2016.
[15] S.A. Ali, A.P. Nutman, K. J. Aswad and B.G. Jones, "Overview of the Tectonic Evolution of the Iraqi Zagros Thrust Zone: Sixty Million Years of Neotethyan Ocean Subduction," *Journal of Geodynamics*, vol. 129, pp. 162–177, 2019.
[16] A.M.M. Aqrawi, "Petrochemistry and Petrogenesis of Ultramafic and Gabbroic Rock Around Mawat Ophiolite Complex, Northeastern Iraq," Unpublished M.Sc. Thesis (in Arabic), University of Mosul, p. 155, 1990.
[17] I.K. Abdulzahra, "Petrology , Geochemistry and Petrogenesis of Gabbroic Rocks (Central Sector) of Mawat Ophiolite Complex, NE Iraq," Unpublished M.Sc. Thesis, University of Baghdad, p. 119, 2008.
[18] T.A. Mirza, "Petrogenesis of the Mawat Ophiolite Complex and the Associated Chromitite, Kurdistan Region, NE Iraq," Unpublished Ph.D. Thesis, University of Sulaimani, p. 250, 2008.
[19] S.Z. Jassim, "Geology of the Central Sector of the Mawat Igneous Complex, Northeastern Iraq," *Journal of Geological Society of Iraq*, vol. 6, pp. 83-92, 1973.
[20] K.J. Aswad, "Arc-continental Collision in Northeastern Iraq as Evidence by the Mawat and Penjwen Ophiolite Complex," *Rafidain Journal of Science*, vol. 10, pp. 51-61, 1999.
[21] H.M. Al-Mehaidi, "Tertiary Nappes in Mawat Range, NE Iraq," *Journal of Geology Society Iraq*, vol. 7, pp. 31-44. 1975.
[22] K.J. Aswad and E.M. Elias, "Petrogenesis, Geochemistry and Metamorphism of Spilitized Subvolcanic Rocks of the Mawat Ophiolite Complex, NE Iraq," *Ofioliti*, vol. 13, pp. 95-109, 1988.
[23] P.G. Jeffery and D. Hutchison, *Chemical Methods of Rock Analysis. Pergamon Series in Analytical Chemistry, Pergoman Press*, 1981, p. 380.
[24] I.K. Al-Saffi, A. Hadi, and A.M.A. Aqrawi, "Petrology of Gabbroic Rocks of Mawat Ophiolite Complex (Central Sector), NE Iraq," *Iraqi bulletin of geology and mining*, vol. 8, no.2, pp. 65-85, 2012.
[25] M.B.M. Zekaria, "Petrology and Geochemistry of the Southern Part of Mawat Ophiolite Complex, Northeastern Iraq," Unpublished M.Sc. Thesis (in Arabic), University of Mosul, p. 85, 1992.
[26] F.H. Hatch, A.K. Wells and M.K. Wells, *Petrology of the Igneous Rocks,12th edition. Thomas Murby, London*, 1961, p. 515.
[27] M.E. Al-Hassan, "Petrology, Mineralogy, and Geochemistry of Penjwin Igneous Complex, Northeast Iraq," Unpublished Ph.D. Thesis, University of Dundee, p. 300, 1982.
[28] R.G. Colleman, *Ophiolites: Ancient Oceanic Lithosphere*, *New York, Springer-Verlag*, 1977, p. 229.
[29] K.G. Cox, J.D. Bell and R.J. Pankhurst, *The Interpretation of Igneous Rocks, George Allen & Unwin, London*, 1979, p. 450.
[30] S.E. Humphris and G. Thompson, "Trace Element Mobility During Hydrothermal Alteration of Oceanic Basalts," *Geochimica et Cosmochimica Acta*, vol. 42, pp. 127-136, 1978.
[31] J.R. Cann,. "Rb, Sr, Y, Zr, and Nb in Some Ocean Floor Basaltic Rocks," *Earth and Planetary Science Letters*, vol. 10, pp. 7-11, 1970.
[32] M.I. Kakar, K. Mahmood, M. Khan, A.K. Kasi and R. Abdul Manan, "Petrology and Geochemistry of Gabbros from the Muslim Bagh Ophiolite: Implications for their Petrogenesis and Tectonic Setting," *Journal of Himalayan Earth Sciences*, vol. 46, no. 1, pp. 19-30, 2013.
[33] O. Parlak, H. Yilmaz and D. Boztug, "Origin and Tectonic Significance of the Metamorphic Sole and Isolated Dykes of Divrii Ophiolite (Sivas, Turkey): Evidence for Break-off Prior to Ophiolite Emplacement," *Turkish Journal of. Earth Sciences*, vol. 15, no. 1, pp. 25-45, 2006.
[34] M. Wilson, *Igneous Petrogenesis: A Global Tectonic Approach, Unwin Hyman, London*, 1989, p. 466.
[35] O. Bektas, Y. Eyoboglu, C. Sen, and B. Rojay, "Reversely Zoned Alaskan-type Mafic-Ultramafic Cumulates in the Eastern Pontide Magmatic Arc, NE Turkey," *Geophysical Research Abstracts*, vol. 9, pp. 01036, 2007.

[36] M. Aditi, R. Arijit, D. Mayukhee and P.P. Sankar, "Petrology, Geochemistry of Hornblende Gabbro and Associated Dolerite Dyke of Paharpur, Puruliya, West Bengal: Implication for Petrogenetic Process and Tectonic Setting," *Journal of Earth System Science*, vol. 121, no. 3, pp. 793-812, 2012.
[37] J.F. Davies, R.W.E. Grant and R.E.S. Whitehead, "Immobile Trace Elements and Archean Volcanic Stratigraphy in the Timmins Mining Area, Ontario," *Canadian Journal of Earth Sciences*, vol. 16, pp. 305-311, 1979.
[38] T.J. Barrett and W.H. MacLean, "Chemostratigraphy and Hydrothermal Alteration in Exploration for VHMS Deposits in Greenstone and Younger Volcanic Rocks," *Geological Association of Canada*, vol. 11, pp. 433-467, 1994.
[39] S. Sun and W. McDonough, "Chemical and Isotopic Systematics of Oceanic Basalts: Implications for Mantle Composition and Processes," *Geological Society London, Special publication*, vol. 42, pp. 313-345, 1989.
[40] C.J. Hughes, *Igneous Petrology, Elsevier Scientific, Amsterdam*, 1982, p. 550.
[41] J.A. Pearce and M.F.J. Flower, "The Relative Importance of Petrogenetic Variables in Magma Genesis at Accreting Plate Margins: a Preliminary Investigation," *Journal of the Geological Society, London*, vol. 134, pp. 103-127, 1977.
[42] J.S. Beard, "Characteristic Mineralogy of Arc Related Cumulate Gabbros: Implications for the Tectonic Setting of Gabbroic Plutons and for Andesite Genesis," *Geology*, vol. 14, pp. 848-851, 1986.
[43] E. Sarifakioglu, H. Ozen and J.A. Winchester, "Petrogenesis of the Refahiye Ophiolite and its Tectonic Significance for Neotethyan Ophiolites Along the Izmir-Ankara-Erzincan Suture Zone," *Turkish Journal of Earth Sciences*, vol. 18, pp. 187-207, 2009.
[44] L. Beccaluva, P. Digirolamo, G. Macciotta and V. Morra, "Magma Affinities and Fractionation Trends in Ophiolites," *Ofioliti*, vol. 8, pp. 307-323, 1983.
[45] K.M. Shamim, T.E. Smith, M. Raza and J. Huang, "Geology, Geochemistry and Tectonic Significance of Mafic-Ultramafic Rocks of Mesoproterozoic Phulad Ophiolite Suite of South Delhi Fold Belt, NW Indian Shield," *Gondwana Research*, vol. 8, no. 4, pp. 553-566, 2005.
[46] S.A. Ali and Z. Rostum, "Petrography and Geochemistry of Gabbroic Rock from the Penjwin Ophiolite, Kurdistan Region, Northeastern Iraq," *Iraqi Geological Journal*. vol. 54, no. 2E, pp. 24-37, 2021.
[47] J.A. Pearce, S.J. Lippard and S. Roberts, "Characteristics and Tectonic Significance of Supra-Subduction Zone Ophiolites," *Geological Society, London, Special Publications*, vol. 16, pp. 77-89, 1984.
[48] M. Shawna, R.O. Maxeiner, and K.M. Ansdell, "Petrography and Geochemistry of Love Lake Lecogabbro, Swan River Complex, Peter Lake Domain, Northern Saskatchewan," *Saskatchewan Geological Survey*, vol. 2, pp. 1-17, 2003.
[49] G. Duclaux, R.P. Menot, S. Guillot, Y. Agbossoumonde and N. Hilairet, "The Mafic Layered Complex of the Kabye' Massif (North Togo and North Benin): Evidence of a Pan-African Granulitic Continental Arc Root," *Precambrian Research*, vol. 116, pp. 101-118, 2006.
[50] J.D. Winter, *An Introduction to Igneous and Metamorphic Petrology, Prentice Hall*, 2001, p. 697.
[51] L. Beccaluva, G. Maccciotta, G.B. Piccardo and O. Zeda, "Clinopyroxene Composition of Ophiolite Basalts as Petrogenetic Indicator," *Chemical Geology*, vol. 77, pp. 165-182, 1989.
[52] D.A. Wood, "The Application of a Th-Hf-Ta Diagram to Problems of Tectono-Magmatic Classification and to Establishing the Nature of Crustal Contamination of Basaltic Lavas of the British Tertiary Volcanic Province," *Earth and Planetary Science Letters*, vol. 50, no. 1, pp. 11-30, 1980.
[53] G.A. Jenner, G.R. Dunning, J. Malpas, M. Brown and T. Brace, "Bay of Islands and Little Port Complexes, Revisited: Age, geochemical and isotopic evidence confirm supra-subduction zone origin," *Canadian Journal of Earth Sciences*, vol. 28, pp. 135-162, 1991.
[54] E.D. Mullen, "A Minor Element Discriminant for Basaltic Rocks of Oceanic Environment and its Implications for Petrogenesis," *Earth and Planetary Scientific Letters*, vol. 62, pp. 53-62, 1983.
[55] J.A. Pearce and J.R. Cann, "Tectonic Setting of Basic Volcanic Rocks Determined Using Trace Element Analyses," *Earth and Planetary Science Letters*, vol. 19, pp. 290-300, 1973.

[56] L.E. Johnson and P. Fryer, "The First Evidence for MORB-like Lavas from the Outer Mariana Forearc: Geochemistry, Petrography and Tectonic Implications," *Earth and Planetary Science Letters*, vol. 100, pp. 304-316, 1990.
[57] J.W. Shervais, "Ti-V Plots and the Petrogenesis of Modern and Ophiolitic Lavas," *Earth and Planetary Science Letters*, vol. 59, pp. 101-18, 1982.
[58] R. Laurent and R. Hebert, "The Volcanic and Intrusive Rocks of the Quebec Appalachian Ophiolites (Canada) and their Island Arc Setting," *Chemical Geology*, vol. 77, pp. 287-302, 1989.